

# Raman scattering investigation on structural and chemical disorder generated by laser ablation and mechanical microindentations of InSb single crystal

M. R. Joya and P. S. Pizani<sup>a)</sup>

*Departamento de Física, Universidade Federal de São Carlos, Caixa Postal 676, 13 565-905 São Carlos, São Paulo, Brazil*

R. G. Jasinevicius

*Departamento de Engenharia Mecânica, Escola de Engenharia de São Carlos, Universidade de São Paulo, C.P. 369, CEP 13566-590 São Carlos, São Paulo, Brazil*

R. E. Samad, W. de Rossi, and N. D. Vieira, Jr.

*Instituto de Pesquisas Energéticas e Nucleares, Centro de Laser e Aplicações, Avenida Professor Lineu Prestes, 2242, Cidade Universitária, 05508-900 Butantã, São Paulo, São Paulo, Brazil*

(Received 14 February 2006; accepted 30 June 2006; published online 14 September 2006)

This paper reports on a topographic and tomographic Raman scattering study of the structural and chemical disorders generated by microindentations in indium antimonide. Two different microindentation mechanisms were investigated: mechanical and laser ablations. In the mechanical indentation, three main effects were observed: amorphization, structural pressure induced phase transition from zinc blende to wurtzite structure, and the presence of both compressive and tensile residual strains. On the other hand, an intense irreversible chemical disorder in the laser ablation was observed, the main effect being the segregation of crystalline antimony up to the surface of the indentation mark. © 2006 American Institute of Physics. [DOI: [10.1063/1.2345052](https://doi.org/10.1063/1.2345052)]

## I. INTRODUCTION

Vickers indentations are primarily used to determine material's hardness and are a measure of its yield or flow stress.<sup>1,2</sup> However, the process of indentation involves interesting physical transformations such as pressure induced structural phase transition, material plastic extrusion, amorphization, and structural defect generation.<sup>3–5</sup> For brittle materials a detailed analysis of the response to mechanical indentation serves as a guide to define the best conditions for machining in ductile regime, in a single point diamond turning machine, for example. This mechanical process of matter removal can be used as an alternative to machine special surface forms, as aspherical silicon lenses for infrared region.<sup>6</sup>

Another more recent route to obtain special surface forms makes use of the fusion process of the material by a high power pulsed laser—laser ablation. In this case the vaporized material during a few picoseconds is removed by a gas flow. These two essentially different processes of matter removal—one purely mechanical and the other purely thermal—lead both to deleterious structural damages to the processed surface.

In the present paper we performed a detailed Raman scattering study on the structural and chemical disorder effects produced into and around the fingerprint of Vickers microindentation and by the laser ablation (“laser indentation”) using a high power pulsed laser in crystalline indium antimonide InSb. The choice for InSb is that among the III-V semiconductors it is the one with the lowest transition pres-

sure value and presents the largest plasticity prior to the onset of brittle failure when mechanically deformed. A topographic study was performed by micro-Raman spectroscopy within and around the vicinity of the indentation marks as well as a tomographic study by using several different exciting wavelengths aiming at investigating in depth the structural damages.

## II. EXPERIMENTAL DETAILS

The samples used in this study were wafers of commercial undoped InSb single crystals grown in the [001] direction. This direction was chosen because in Raman scattering experiments, in the backscattering configuration with the incident and scattered light along [001] direction, the Raman spectrum presents only a single peak at  $190\text{ cm}^{-1}$  due to the light scattering by the longitudinal optical (LO) phonon, as previewed by the Raman selection rules for the zinc blende structure of InSb. The presence of the peak at  $180\text{ cm}^{-1}$  due to the light scattering by the transverse optical (TO) phonon and the broadening of the Raman peaks indicate structural disorder. So, the intensity ratio between the TO and LO Raman peaks can be used to probe the structural disorder of InSb. Furthermore, residual strains can be probed by the shift of the Raman peaks: positive (negative) shifts indicate compressive (tensile) residual strain.

The Raman scattering measurements were performed using a micro-Raman spectrometer with a triple monochromator and a charge-coupled device (CCD) detector. As exciting wavelengths were used, several lines of an Ar<sup>+</sup>–Kr<sup>+</sup> ion laser, ranging from 458 to 647 nm, focused on the sample as a spot of about  $1\text{ }\mu\text{m}^2$  by a microscope with a

<sup>a)</sup>Electronic mail: pizani@df.ufscar.br

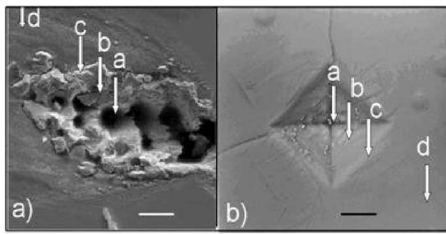


FIG. 1. Scanning electron microscopy of the (a) Vickers indentation and (b) laser ablation of InSb. The arrows (a)–(d) indicate the points where the Raman spectra were performed, shown in Figs. 2 and 5. The bars correspond to 5  $\mu\text{m}$  in (a) and 10  $\mu\text{m}$  (b).

100 $\times$  objective. The penetration depth of the light of these lines can be obtained if the optical coefficient is known. However, the estimation of the penetration depth of the light in our case is not so easy, because we do not know the degree of structural disorder at different positions of indentation marks, only at the center of the mechanical indentation, where the InSb is completely amorphous when sampled with the 458 nm line. From the paper of Ojima and Adachi, in which the dielectric function of amorphous InSb was measured, we estimated the absorption coefficient ( $\alpha$ ) between 0.08 and 0.05  $\text{nm}^{-1}$  for the 458 and 647 nm excitation lines, respectively.<sup>7</sup> These values lead to the penetration depth ( $\sim 1/\alpha$ ) of about 12 and 20 nm, respectively. For crystalline InSb, these values are about 17 and 36 nm.<sup>8</sup> Finally, all measurements were performed at room temperature, with the laser power kept at about 1 mW at the entrance of the microscope to avoid thermal effects on the spectra. All results were obtained from fitting the Raman peaks using Lorentzian line shapes.

The microindentation tests were performed in a VMHT MET Leica (Leica Mikrosysteme, GmbH; A-1170, Vienna, Austria) microindentation apparatus using a Vickers pyramidal indenter. The indentation load used in the tests was 25 g. The microindentation test was performed on  $12 \times 12 \text{ mm}^2$ , 0.5 mm thick samples of monocrystalline InSb. Vickers pyramidal indenter was employed having centerline-to-face angle 68°. The indentation speed was 60 m/s and the holding time of 15 s was used. The results presented in this work were performed in four different sites: (a) at the center of the indentation mark, (b) at the middle of the indentation four face, (c) at the border of the mark, and (d) at 20  $\mu\text{m}$  distant from the indentation mark, shown in detail in Fig. 1.

The laser indentations were performed using ultrashort laser pulses from a Quantronix Odin CPA system seeded by a Coherent Mira-SEED. Only one laser pulse was used for each indentation; the temporal pulse width was 60 fs and energy  $E=167 \text{ mJ}$ . The laser pulse was focused on the crystal surface by an  $f=90 \text{ mm}$  converging lens to produce a spot with approximated intensity of  $7.3 \text{ TW/cm}^2$ . The experiment, which was performed in air, produces a  $10 \times 30 \mu\text{m}^2$  elongated “scratch” on the surface of the sample.

### III. RESULTS AND DISCUSSIONS

#### A. Mechanical indentations

Figure 2 shows a sequence of Raman spectra performed from the center of the indentation (a) to points far about

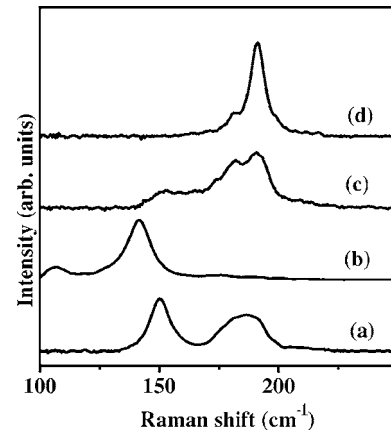


FIG. 2. Raman spectra performed on points at the center of the fingerprint (a), at the center of the face (b), at the border (c), and far from the fingerprint (d), using the 458 nm exciting wavelength, whose penetration depth of the light is between 12 (for amorphous InSb) and 17 (crystalline InSb) nm.

20  $\mu\text{m}$  from the border (d), using the line of 458 nm, with penetration depth between 12 and 20 nm. Compared with the Raman spectra of the crystalline InSb (d), several different effects can be seen: the excitation of the TO mode of the InSb inside the indentation with the simultaneous broadening of the LO peak, the amorphization of InSb in the region around the center, denounced by the presence of the broad band at  $185 \text{ cm}^{-1}$  (the optical band, which reflects the optical vibrational density of states), positive and negative frequency shifts of both LO and TO modes, and the appearance of new Raman peaks at the center of the face of the fingerprint. The activation of the TO peak and the broadening of the LO indicate high structural disorder of the zinc blende phase of InSb due to the defect generation, driven by the high pressure with high shear components applied by the indenter. At the center of the indentation, where the applied pressure is maximum, a complete amorphization of the material can be observed.

In relation to the residual strains, denounced by the shifts of the Raman peaks, there is an interesting behavior of InSb which shows positive and negative frequency shifts along the indentation face, similar to that also observed in GaAs, but completely different from the Si case, in which only compressive residual strains was observed, with very high values at the border of the indentation.<sup>9,10</sup> Figure 3 displays the relative frequency shift of the LO mode ( $\Delta\omega = \omega - \omega_0$ , where  $\omega_0$  is the frequency of the LO mode far from indentation) for several different positions from far until to the center of the indentation. Around the center of the triangular face of the indentation there is an inversion of the sign of the residual strain, changing from compressive to tensile. In this region two new intense features appear in the Raman spectra at about 105 and  $140 \text{ cm}^{-1}$ , suggesting that a structural phase transition occurred. These features are indicative of the occurrence of a pressure induced structural phase transition from zinc blende to wurtzite structure. The frequency shift of the peak from  $140 \text{ cm}^{-1}$  in Fig. 2(b) to  $150 \text{ cm}^{-1}$  in Fig. 2(a) can be attributed to strains and/or disorder effects. Similar features were also observed by Kailer *et al.* in indented InSb but only in cases where the decompression rate was inten-

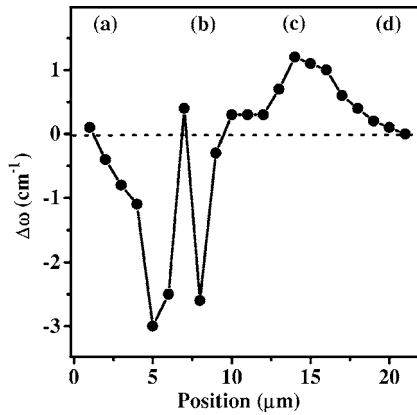


FIG. 3. Frequency shift of the LO mode for several positions, from the center of the indentation to points far from the indentation: at the center of indentation (a), at the center of the face (b), at the border (c), and far from the fingerprint, at about 20  $\mu\text{m}$  from the center (d).

tionally increased, contrary to our case.<sup>11</sup> Such a structural phase transition was also predicted in theoretical studies reported by Wang and Ye, in which this phase transition could occur around 1.85 GPa.<sup>12</sup> To confirm this theoretical prediction, we carried out careful measurements applying hydrostatic pressure using a diamond anvil cell monitored by Raman scattering, and no specific phase transition was observed at this level of hydrostatic pressure.

Figure 4 shows the same above sequence of Raman spectra, but now using the 647 nm as excitation line, with penetration depth between 20 and 30 nm. It can be noticed that the LO Raman peak at about 190  $\text{cm}^{-1}$  is always more intense than the TO one, indicating that the structural disorder decrease increases the probed depth, being localized mainly into the first 12 nm. The intense Raman peaks of the wurtzite phase are still present around the center of the face. At the center of the indentation, the structural disorder of the zinc blende phase is maximum.

## B. Laser indentations

Figure 5 shows a sequence of Raman spectra probed in different sites, from the center to points distant from the laser

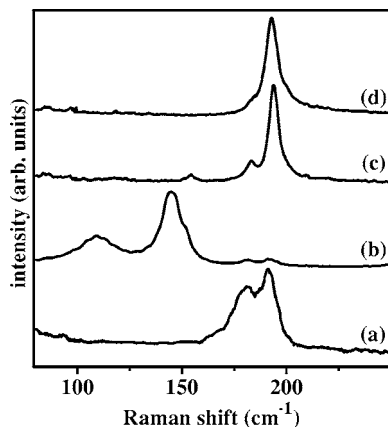


FIG. 4. Raman spectra performed on points at the center of the fingerprint (a), at the center of the face (b), at the border (c), and far from the fingerprint (d), using the 647 nm as exciting wavelength, whose penetration depth of the light is between 20 (amorphous) to 36 (crystalline) nm.

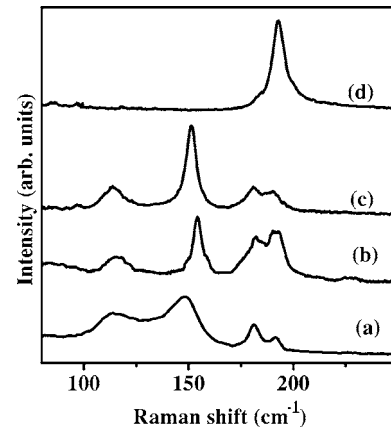


FIG. 5. Sequence of Raman spectra along a line starting at the center (a) to points far from (d) the center of the laser indentation. (e) is the Raman spectrum of a polycrystalline sample of Sb.

indentation, as shown in Fig. 1. Within the indentation, from (a) to (b), the Raman spectra show not only the activation of the TO mode, indicating structural disorder of the zinc blende phase of InSb, but also features at 115 and 154  $\text{cm}^{-1}$ . These Raman peaks are characteristic of the presence of crystalline antimony and can be confirmed when compared with the spectrum of polycrystalline Sb, shown in Fig. 6(e). This topographical analysis demonstrated that the thermal process of material removal leads to both chemical and structural disorders. In elemental semiconductors such as Si, these effects are easily overcome by thermal annealing. However, for III-V semiconductors these disorder effects are very difficult to be overcome because thermal annealing also leads to chemical disorder.

Figure 6 shows a sequence of Raman spectra probed at the same site within the laser indentation, nevertheless with different excitation wavelengths, aiming at probing in-depth disorder. It is worth noticing the increase in the intensity of the  $A_{1g}$  and  $E_g$  Raman peaks of antimony relative to that of InSb, with decreasing excitation wavelength, i.e., with the decrease of penetration depth. This result indicates that the localization of the antimony is mainly in the outmost surface vicinity. Similar results were reported for GaSb and GaAs undergone to heat treatment in conventional furnace, where

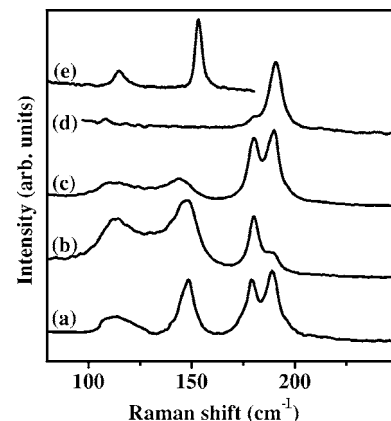


FIG. 6. Raman spectra taken at the same point of the laser indentation with different excitation wavelengths: (a) 466, (b) 488, (c) 514, and (d) 647 nm. In (e) the Raman spectrum of a polycrystalline sample of Sb is displayed.

the migration of the V element to the surface was detected.<sup>13</sup> Furthermore, the negative frequency shifts of the  $A_{1g}$  and  $E_g$  modes of antimony crystallized in the surface relative to the bulk reveals an important compressive strain. The maximum frequency shift of the  $A_{1g}$  mode, about  $7\text{ cm}^{-1}$ , occurs for the line of 488 nm, as shown in Fig. 6(b), whose penetration depth is about 18 nm. Using the results from Ref. 14, the residual stress can be estimated to be about 1.5 GPa.

#### IV. SUMMARY AND CONCLUSIONS

We have performed a detailed Raman scattering study on the disorder effects generated by indentations of InSb using two different mechanisms: mechanical microdeformation and thermal fusion. Our Raman results showed that the mechanical mechanism has led to high structural disorder, localized mainly at about 12–17 nm into the surface and a complete amorphization at the center of the indentation. At the center of the face of the indentation mark generated by the pyramidal indenter, there are two very interesting effects: a change in sign of the residual strain, changing from compressive to tensile, and a pressure induced phase transition from zinc blende to wurtzite structure. The thermal fusion mechanism produced other effects. Raman results indicated that the thermal fusion mechanism has led to both structural disorder in the zinc blende phase of InSb and chemical disorder, with the migration of the antimony crystallized in the

outmost surface vicinity. Moreover, the antimony is submitted to a maximum residual stress of about 1.5 GPa, and it is at about 18 nm distant from the surface. Finally, our results indicate that both mechanical and thermal processes lead always to deleterious disorder effects, considering to be a limiting factor to the use of the mechanical machining and laser ablation of special surfaces in III-V semiconductors, contrary to the elemental semiconductor as Si, where the structural disorder effects can be easily removed by thermal annealing.

<sup>1</sup>A. P. Gerk and D. Tabor, *Nature (London)* **271**, 732 (1978).

<sup>2</sup>C. A. Schuh, *Mater. Today* **9**, 32 (2006).

<sup>3</sup>D. R. Clarke, M. C. Kroll, P. D. Kirchner, R. F. Cook, and B. J. Hockey, *Phys. Rev. Lett.* **60**, 2156 (1988).

<sup>4</sup>G. M. Pharr, W. C. Oliver, and D. S. Harding, *J. Mater. Res.* **6**, 1129 (1991).

<sup>5</sup>A. Jayaraman, W. Klement, and G. C. Kennedy, *Phys. Rev.* **130**, 540 (1963).

<sup>6</sup>K. E. Puttick, *J. Phys. D* **13**, 2249 (1980).

<sup>7</sup>T. Ojima and S. Adachi, *J. Appl. Phys.* **82**, 3105 (1997).

<sup>8</sup>D. E. Aspnes and A. A. Studna, *Phys. Rev. B* **27**, 985 (1982).

<sup>9</sup>P. Puech, F. Demangeot, and P. S. Pizani, *J. Mater. Res.* **19**, 1273 (2004).

<sup>10</sup>P. Puech, F. Demangeot, P. S. Pizani, S. Wey, and C. Fontaine, *J. Mater. Res.* **18**, 1474 (2003).

<sup>11</sup>A. Kailer, K. G. Nickel, and Y. G. Gogotsi, *J. Raman Spectrosc.* **30**, 939 (1999).

<sup>12</sup>S. Q. Wang and H. Q. Ye, *J. Phys.: Condens. Matter* **14**, 9579 (2002).

<sup>13</sup>C. E. M. Campos and P. S. Pizani, *Appl. Surf. Sci.* **200**, 111 (2002).

<sup>14</sup>C. E. M. Campos and P. S. Pizani, *J. Appl. Phys.* **89**, 3631 (2001).